

Object orientation and visualization of physics in two dimensions

Mark Burgess, Hårek Haugerud and Are Strandlie

*Centre of Science and Technology, Faculty of Engineering, Oslo College, 0254 Oslo, Norway
and*

Institute of Physics, University of Oslo, P.O.Box 1048 Blindern, 0316 Oslo, Norway

(April 29, 2021)

We present a generalized framework for cellular/lattice based visualizations in two dimensions based on state of the art computing abstractions. Our implementation takes the form of a library of reusable functions written in C++ which hides complex graphical programming issues from the user and mimics the algebraic structure of physics at the Hamiltonian level. Our toolkit is not just a graphics library but an object analysis of physical systems which disentangles separate concepts in a faithful analytical way. It could be rewritten in other languages such as Java and extended to three dimensional systems straightforwardly. We illustrate the usefulness of our analysis with implementations of spin-films (the two-dimensional XY model with and without an external magnetic field) and a model for diffusion through a triangular lattice.

I. INTRODUCTION

Although computer simulations of many physical systems are common for computing specific quantities, they do not necessarily give a direct and overall impression of the dynamics of the systems under a variety of conditions. What is often lacking from the physicist's repertoire is the possibility of a direct visualization of the behaviour of microscopic systems in some appropriate semi-classical limit. Such a mental image of the mechanics of the problem can be a source of great inspiration, both for understanding established problems, and for designing new scenarios. The ability to vary initial and boundary conditions (temperature, external field and any other external parameters) and compare several simulations has enormous potential for the comprehension of the qualitative behaviour, while at the same time enabling quantitative information to be calculated and displayed along side.

In recent years the status of two dimensional physics has changed from being mathematical idealization to being a realistic physical prospect. The fractional quantum Hall effect and high temperature superconductivity are widely believed to be two-dimensional phenomena to a good approximation. Moreover developments in the growth of ultra-thin layered heterostructures makes the modeling of two-dimensional systems ever more important.

Theoretical developments in two dimensional physics have generated a large body of work. Notable topics include the notion of fractional statistics [1] or anyons (particles which interpolate between Bose-Einstein and

Fermi-Dirac statistics), anyon superconductivity and layered systems as potential models for the new high temperature superconductors, the quantum Hall effect and spin textures, to name but a few [2]. Many of these models could profitably be simulated visually to gain an intuitive picture of what takes place. There are many other interesting candidates for visual models in two dimensions: including the study of fields in waveguides and cavities (the micromaser) and spin computers [3–10]. Spin diodes [11] have been studied both experimentally and theoretically and could profitably be made into a visual simulation.

Recently several groups have begun to appreciate the importance of direct visualization in 2-dimensional systems. Since direct experimental observations are difficult to achieve, and certainly difficult to repeat under identical conditions, computer simulations are an obvious and valuable surrogate. Computer visualization always involves some form of compromise or approximation, and sufficient control of these compromises is an important concern, but the bonus of a concrete dynamical picture of a physical system often outweighs minor qualms about their accuracy. Graphical representation of data places heuristic understanding before precision.

Certain physical situations are ideally suited to visualization. For example: any kind of field, be it of a scalar or vector character, with arbitrarily complicated boundary conditions, is easily rendered visually, but might be described by complicated special functions algebraically or numerically, making it difficult to gain a qualitative understanding.

In this article, we present a visualization scheme for 2 dimensional systems and layered 3 dimensional systems which may be used to play physical simulations on a lattice like a one-way video recording. Initial and boundary conditions may be edited, and parallel simulations employing different parameters may be compared. The framework is general, but we choose to illustrate it by looking at 2 dimensional spin systems and diffusion models, which provide a perfect illustration of the principles.

II. CELLULAR AUTOMATON SIMULATION ENVIRONMENT (CASE)

A convenient framework on which to base a system of visualization is the cellular automaton. The idea of cellular automata was introduced around 70's and 80's

with key papers by among others Wolfram. For a review, with references, see ref. [12]. A cellular automaton may be thought of as a simulation engine in which cells, (or lattice plaquettes) arranged in a symmetrical pattern, interact with their neighbours according to well-defined rules. Each cell or site has a number of variables associated with it, describing the state of the system at that point (e.g. temperature, occupation number, spin state etc), and that state evolves in time according to a supplied rule which embodies the dynamics of the model. A suitable visual representation of the automaton can be constructed by choosing a property like colour to represent temperature (or other scalar quantities) and arrows to represent vector quantities. Combinations of these, together with the ability to limit and change the variable being displayed, allow complex models to be visualized in detail.

Cellular automata have traditionally been used by physicists and biologists for studying such diverse problems as the development of cellular life, mixing of fluids, penetration of porous media, magnetic spin systems etc. Any system in which space and time can be discretized into an appropriate lattice can be modeled by a suitably complicated automaton and this is in tune with the unavoidable granulization which any system must undergo in a visualization. Increasingly cellular automata are being used as simulated ‘analogue computers’ by engineers and statisticians. They are used in the modeling of traffic flow at junctions, electrical networks, and the diffusion of gases and spreading of interfaces, to name but a few applications. It has been recently shown that there is a connection between cellular automata and the N -soliton problem which is of direct interest in non-linear optics as well as other fields [20]. By adopting a generalized cellular automaton for our simulation environment, we must introduce only one pertinent restriction: namely that simulations are always pinned to a predefined lattice [21].

III. ABSTRACTION

The most important technical feature of the CASE library is its object orientated construction. Object orientation is about hiding details inside ‘black-boxes’ so that they do not interfere with the natural logical structure of a problem. It is also about separating independent issues in a program in a disciplined way. Using an object orientated philosophy together with the polymorphism allowed by C++, we are able to create models with a structure which is independent of low-level details. By low level details we refer to both microscopic physical details of the models we simulate and low level programming details, such as the specifics of how to draw graphics in windows. The object model is a powerful abstraction which had largely been ignored by physicists who are more used to nuts and bolts programming with

languages like FORTRAN. We feel that this aspect of CASE should not be underestimated. Practical models of real physics in complex systems will only succeed in the future if there is a serious attempt to deal with this complexity in a logical and organized manner.

As an example of the benefits which object orientation offers, we can note the following. Normally cellular automata in two dimensions live on a square lattice. In our framework we have been careful to admit the possibility for models to employ any regular tessellating lattice. We do this by separating issues which concern the lattice structure from as much as possible of the remainder of the program, and vice versa. In many cases we can code physical models in a way which is independent of the underlying symmetry of the lattice by referring only to generic concepts such as nearest neighbours. The knowledge of how to locate nearest neighbours can be hidden inside a black box associated with a particular symmetry. This allows us to model crystalline structures with hexagonal and other symmetry groups simply by replacing one black box with another. CASE is not simply a two dimensional graphics rendering package. The library is not just about making available different geometries. It is also about simplifying and rendering different physical concepts. Any useful visualization technology must be based on general, reusable abstractions which make physical understanding paramount. Our approach is based on a fundamental untangling of concepts associated with two dimensional cellular automata.

Figure 1 shows the way in which we have chosen to separate the issues in the CASE library. The structure of objects and the way in which they relate to one another have been designed with a practical eye: we are looking to write real computer programs, not merely theoretical constructs. The top of the hierarchy is therefore the coarsest object in our scheme: an application, or complete program. The application part of our scheme is a framework in which we can open one or more simulations and run them concurrently, even in parallel. An application contains convenient control switches for starting and stopping simulations and keeping them synchronized with one another.

Beneath the application layer is the model layer. A model is a box which encapsulates everything about a given physical system, such as the rules by which physics is done. We can think of this part of the model as defining the Hamiltonian for the system, since the rules of how the system develops in time reside in this structure. This black box is itself built out of component objects which have a more general validity than one single model. For instance, ‘Environment’ describes the symmetry of the lattice and the way in which one cell relates to the others. This is analogous to the symmetry group of the lattice and its boundary conditions (periodic, twisted, or isolated identification of the edges). A ‘Cell’ object is a capsule which contains all of the physical variables which are required by the physical model at every site on the lattice. This is analogous to the choice of variables in the

Hamiltonian, or the parameterization of the problem. Finally we have some strictly technical objects which have to do with the visual mechanisms of the computer and the definition of re-usable symbols for representing the physical variables contained in cells.

This object abstraction covers a complete classification of properties associated with physical systems in a rational, formalized scheme. We can define plug-in visualization schemes for scalar, vector or other data based on a lattice of arbitrary symmetry. We can render these properties with arbitrary shapes and colours or even with numerical values, or combinations of these objects. Visual objects might hide variables which can be revealed by clicking on a cell to avoid visual clutter. Perhaps more importantly than the results, we are able to program the physics in a way which preserves the structure of a system at the algebraic level: cells are the basic dynamical variables, models are the Hamiltonian, and each of these can be separated, without muddling issues.

CASE	Symbol	Meaning
Update()	H	Hamiltonian
Cell object	ϕ	The field
Environ	\mathcal{G}	Symmetry group
Property	T, E, S	Physical quantities

The basic symbol types which have been used so far are in example models are: coloured blobs to represent scalar values, arrows (with variable size) to represent vector data and the use of scaled and coloured plus and minus symbols to represent the locations of positive and negative charges of varying magnitudes, particularly in connection with vortices or charges.

IV. IMPLEMENTATION

The CASE simulation environment was began in Oslo in 1993 [22] with a simple implementation of the XY-model programmed as a one-off application on a unix workstation, using the X11 windowing library [23]. Since then, we have developed a generalized framework for cellular or lattice based visualizations, based on state of the art, freely distributable computing systems [24,25].

Our aim has been to create a flexible system for constructing generalized, visual models sufficient for our own special needs, but which may be adopted and developed by others, without the need for expensive software packages. Indeed all of the tools required to use our models are freely available on the internet. Our code is written in object-oriented C++ and is designed carefully to be comprehensible and reusable by the physics community. The technical details of this framework will be published elsewhere [24]. CASE takes the form of a library of reusable functions which hide complex programming issues from the user. We envisage our user to be an intelligent scientist with an aptitude for programming, but

with little patience for incomprehensible graphical window interfaces. The framework may be loosely described as follows:

- CASE supports an N state cellular automaton, based on a lattice with user configurable symmetry. Each site can be edited or randomized to specify initial conditions.
- The method of visualization must be user configurable. Simple mechanisms for adding and changing colour in real-time are provided, for example.
- The size of system and choice of boundary conditions may be changed as run-time parameters.
- Resizing and zooming in and out of the lattice permits the handling of large models.
- Freeze frame and resume, with possibility of saving the state of the simulation for later continuation or analysis. Snapshots may also be sent to a printer or other device.

A. Object construction

The implementation of a model in CASE involves the definition of a model object (which in turn uses reusable cell objects), and all of its methods (functions). Here is an example model object.

```
class XYModel : public CAModel
{
public:

    XYModel();
    XYModel(Widget new_parent);
    ~XYModel();

    virtual void Update();
    virtual void RightClick(double x, double y);

protected:

    virtual void Draw(int cell_index);
    virtual void Redraw();

    virtual void AllocateCells(int new_cells);
    virtual void ReadEnvironRequester();

    void Init_spinconfig();
    int Monte_Carlo(int cell_index);
    double Trial_angle(XYCell *current);
    double New_energy(int cell, double trial_angle);
    double Old_energy(int cell);
    int CheckVortex(int cell_index);
    void CheckVortices();

    CAArrowSymbol *symbol;
```

```

double beta;
Req temp_req;
int iter;

private:
    static void temp_ok(Req *req, XtPointer data);
    static void temp_cancel(Req *req, XtPointer data);
    static void set_temp(Widget w, XtPointer data,
                        XtPointer garb);
};

```

The function prototypes here refer to functions which the user of CASE must supply in order to describe the nature of cells. In addition to certain required functions which control aspects of the user interface, which CASE needs in order to function (`RightClick`, `Update`, etc.), any number of other functions may be created as is convenient for implementing the model. In the XY example, these include `Init_spinconfig`, `CheckVortices` etc.

The most important function is the Update method. This is a formal coding of the Hamiltonian of the system. In many cases this update procedure is based upon randomized statistical processes. This is implemented using a Monte Carlo algorithm.

B. Monte Carlo update procedure

In a statistical system, close to thermodynamic equilibrium, the average state of the system is characterized by a temperature $T > 0$, or equivalently by inverse temperature β . Microscopically, the state is defined by the condition of every spin in the simulation, but this is not a static state: we must allow for fluctuations. Since it is impractical to account for every degree of freedom which gives rise to such fluctuations, one adopts a heuristic algorithm for including them. In our case, this is known as the Metropolis algorithm, which is a variant of so-called Monte Carlo methods.

A Monte Carlo method is a way of using random numbers to update the state of the system (the name Monte Carlo evokes images of gambling). Instead of iteratively parsing the cellular grid and updating state of each cell deterministically, one chooses spins in the grid according to some rule and applies a rule which only updates spins only with a certain probability, characterized by the Boltzmann factor. The algorithm is as follows:

- Select a spin,
- Pick an angle by which the spin might flip at random,
- Compute the energy change associated with the random flip ΔE ,

- Calculate the probability of transition $W = \exp(-\beta\Delta E)$,
- Calculate a random number x between zero and unit,
- if $x < W$, update the spin, otherwise leave it alone.

In a real system, fluctuations cause spins to flip at random. In this sense the Monte Carlo algorithm may be thought of as a true time-dependent simulation of a physical process approaching equilibrium. Note however, that there is no immediate connection between the time elapsed in the simulation and ‘physical time’. The true physical time is modelled most realistically if we update the sites at random, but time is saved if we go through the grid in an orderly fashion. Although one would not expect any major problems to arise from this orderly parsing of the grid, it makes the identification of the physical time a more heuristic than precise procedure. In the limit of large times, the ergodicity of the system should guarantee that the specific method of updating would not play a role in the final outcome. In our example implementation of the XY-Model, we choose random updates to best simulate a physical system.

C. Threads

In the present model we have been able to get away with a rather primitive algorithm for scheduling updates of the window graphics, based on the X timeout mechanism. This method has several failings: if the calculations are very time consuming, then the normal X event loop becomes neglected. This means that the responsiveness of windows and button clicks with degrade and become unacceptably slow. This is likely to be a problem in more ambitious simulations. The only way to avoid this problem is to separate the updating of the window from the business of processing X11 messages. The most natural way to do this is to use threads. By making a simulation multithreaded, we can most efficiently organize the time spent on each task without having to break up the updating algorithm, in an unaesthetic fashion. This is also a natural objection oriented solution to the problem.

CASE currently uses release 6 of X11 and will continue to build on this and later releases. X11R6 contains a thread compatible library which we shall experiment with in the future. One possibility is to use POSIX pthreads, but so far only a few operating systems have implemented pthreads in an acceptable way. We shall most likely try to encapsulate the threading abstraction in a suitable class to hide the chiefly technical difficulties.

V. EXAMPLE VISUALIZATIONS

We illustrate the usefulness of our simulator with examples based on two-dimensional spin-films and a dif-

fusion model. We hope that these model simulations will be of widespread interest to physicists and students alike and lead to many helpful insights into the nature of microscopic systems both in classical, semi-classical and quantum mechanical descriptions. In the first two cases we focus on what can be learned from the visualization of physical systems, while in the final example we demonstrate the benefits of our abstraction policy.

A. The two-dimensional XY model

One of the simplest but nonetheless interesting models in two dimensions is the so-called XY-model for spin systems. This model has been studied many times before in simulations, but to our knowledge never visualized directly. It exhibits vortices and a phase transition and therefore serves as a basic template for all spin models in two dimensions. Considerable efforts have been expended in order to explore the properties of the two-dimensional classical XY model (for a review, see [13]). This has partly been motivated by the fact that the XY model can be viewed as an approximate microscopic model of a neutral two-dimensional superfluid [14] and thus describe physical systems such as ^4He films. Furthermore it is closely related to the two-dimensional Coulomb gas, which is also capable of describing charged superfluids [15]. When including the electromagnetic vector potential in the XY model it can be viewed as an approximate microscopic model for superconducting films as well as for two-dimensional arrays of weakly coupled Josephson junctions [16].

Due to the complexity of the models, analytic solutions are hard to find; one therefore resorts to Monte Carlo simulations to obtain estimates of thermal expectation values [17–19].

The two-dimensional XY model is a model of classical spins \mathbf{S} located at each lattice site of a two-dimensional square lattice with lattice spacing a . The name XY stems from the fact that the spins are constrained to rotate in a plane, and the spins are classical in the way that they can point in any direction in this plane. Originally the model was derived as a simplification of the Heisenberg spin model of ferromagnetism. In the classical Heisenberg model the spins can point in any direction in three-dimensional space.

The basic feature of the model on a microscopic scale is the nearest- neighbour interaction between the spins. The Hamiltonian is given by

$$H = -J \sum_{\langle \mathbf{x}, \mathbf{x}' \rangle} \mathbf{S}_{\mathbf{x}} \cdot \mathbf{S}_{\mathbf{x}'} \stackrel{|\mathbf{S}|=1}{=} -J \sum_{\langle \mathbf{x}, \mathbf{x}' \rangle} \cos(\phi_{\mathbf{x}} - \phi_{\mathbf{x}'}) \quad (1)$$

where $\langle \mathbf{x}, \mathbf{x}' \rangle$ means that the sum is restricted to nearest-neighbours, and J is a positive coupling constant making the coupling ferromagnetic. Here $\phi_{\mathbf{x}}$ means the

angle $\mathbf{S}_{\mathbf{x}}$ makes with an arbitrary, fixed axis. The line between two sites will be denoted a link, and the square region on the inside of four neighbouring links will be denoted a plaquette. An illustration of such a spin lattice is shown in figure 2.

In the CASE setup, this Hamiltonian is coded into a module called XYModel which makes reference to separate cell objects containing angle data. The statistical mechanics of the model is contained in the partition function

$$Z = \int_{-\pi}^{\pi} \prod_{\mathbf{x}} d\phi_{\mathbf{x}} e^{K \sum_{\langle \mathbf{x}, \mathbf{x}' \rangle} \cos(\phi_{\mathbf{x}} - \phi_{\mathbf{x}'})} \quad (2)$$

where $K = \beta J = J/kT$. Any thermodynamic quantity of interest can be calculated through the partition function, or in our case from the Model abstraction.

We now summarize some of the physics of this model. If we transform each spin according to

$$\phi_{\mathbf{x}} \rightarrow \phi_{\mathbf{x}} + \alpha \quad (3)$$

where α is some fixed angle, we see that the Hamiltonian is invariant. The system possesses therefore a continuous symmetry. When $T \rightarrow 0$ all spins will be aligned because of the ferromagnetic interaction, and hence the model has an infinitely degenerate ground state. The ground state configuration is where all spins point in the same direction, thus we expect only small deviations from such a configuration at low temperatures. This means we may write

$$\phi_{\mathbf{x}} - \phi_{\mathbf{x}'} \ll 1, \quad (4)$$

where \mathbf{x} and \mathbf{x}' are neighbouring sites. Furthermore, it suggests that we can expand the cosine in a Taylor series and keep the terms up to second order,

$$\cos(\phi_{\mathbf{x}} - \phi_{\mathbf{x}'}) \simeq 1 - \frac{1}{2}(\phi_{\mathbf{x}} - \phi_{\mathbf{x}'})^2 \quad (5)$$

and thus

$$H = \frac{J}{2} \sum_{\langle \mathbf{x}, \mathbf{x}' \rangle} (\phi_{\mathbf{x}} - \phi_{\mathbf{x}'})^2 \quad (6)$$

Here an unimportant constant term expressing the zero point energy has been discarded.

If we look at the spin system on a large scale, it is not possible to see the microscopic structure. We can therefore approximate the discrete formulation with a continuum model. This is equivalent to letting the lattice spacing approach zero, and hence

$$H = \frac{J}{2} \sum_{\langle \mathbf{x}, \mathbf{x}' \rangle} (\phi_{\mathbf{x}} - \phi_{\mathbf{x}'})^2 \stackrel{a \rightarrow 0}{\rightarrow} \frac{J}{2} \int d^2x (\nabla_{\mu} \phi)^2 \quad (7)$$

where $\mu = 1, 2$. The Hamiltonian is seen to have the same form as the action of a real, one-component, massless field

in 2+0 dimensions. The partition function then becomes the functional integral

$$Z = \int \mathcal{D}\phi e^{-\frac{\kappa}{2} \int d^2x (\nabla_\mu \phi)^2} \quad (8)$$

This changeover from a discrete to continuum model can be simulated in CASE by turning up the number of sites on the lattice. We are also able to zoom in and out of the lattice to compare and contrast the microscopic and the macroscopic.

The field configurations which make the action stationary with respect to small variations of the field can be found as solutions of the Euler-Lagrange equations

$$\frac{\delta H[\phi]}{\delta \phi} = 0 \quad (9)$$

which implies

$$\nabla^2 \phi = 0 \quad (10)$$

By transforming to polar coordinates, two simple solutions are easily guessed

- 1) $\phi = \text{const}$
- 2) $\phi = n \cdot \theta$

Here θ is the polar angle with respect to some origin. The first solution gives us the global energy minimum of the system with all spins aligned. For the second solution there is mathematically no constriction on the real constant n , but the fact that the field strictly is an angle gives

$$\phi(\theta + 2\pi) = \phi(\theta) + k \cdot 2\pi, k \in \mathcal{Z} \quad (11)$$

and hence $n = k$. If n is chosen to be 1, a spin configuration will look like the one shown in figure 3a. This configuration is what is called a vortex. By letting each spin transform according to $\phi \rightarrow \phi + \pi/2$ we still get a solution of the equation, and a typical whirl shows up. This is shown in figure 3b. We expect to find such vortices in a simulation.

We see that, in moving along the whole boundary of the lattice in figure 3a counterclockwise, the spins have undergone one full revolution. If the sites are labeled (x, y) with $(1, 1)$ at the bottom left and $(4, 4)$ at the top right, the sum of spin differences along the boundary is given as

$$S = (\phi_{2,1} - \phi_{1,1}) + (\phi_{3,1} - \phi_{2,1}) + (\phi_{4,1} - \phi_{3,1}) + \dots + (\phi_{1,1} - \phi_{1,2}) = 2\pi \quad (12)$$

with $S = 2\pi$ expressing the fact that the spins have undergone one revolution. In general, evaluating this sum of spin differences along any closed path on a lattice will give some multiple of 2π

$$S = n \cdot 2\pi \quad (13)$$

and this n is the definition of the vorticity or the charge of the vortex. If $n = 0$ there is no vortex inside the loop. If $n \neq 0$, there is a vortex with vorticity n inside the loop. When there are several vortices inside our closed loop, the value of n becomes the total vorticity of the region. The vortex in figure 3a is seen to have $n = 1$, and it follows that a vortex with vorticity n is constructed in the simplest way by letting

$$\phi = n \cdot \theta \quad (14)$$

According to Kosterlitz and Thouless [26] the vortices only exist in tightly bound pairs with opposite vorticity at low temperatures. At some critical temperature, T_c , the first vortex pair unbinds and the vortices are free to move to the one-dimensional surface of the lattice under the influence of an arbitrarily weak, external magnetic field. The phase transition is therefore called the vortex-unbinding transition, and it is characterized by this abrupt change in the response to the magnetic field. Following their argument, the vortices are equivalent to freely moving, straight parallel, current-carrying conductors located at the centres of the vortices. These will therefore tend to move at straight angles to an applied magnetic field in the plane of the system, the direction determined by the direction of the current. This is easily seen by the well-known formula for the force on a current-carrying wire in a magnetic field

$$\mathbf{F} = I \cdot \mathbf{l} \times \mathbf{B} \quad (15)$$

which tells us that the forces on wires with oppositely directed currents are oppositely directed and perpendicular to the field. In the case of a vanishing external magnetic field there are no driving forces on the vortices, but we should still observe free vortices above T_c solely due to thermal fluctuations.

In order to focus on the thermal behaviour of the XY model we use a Monte Carlo simulation, with a standard, local Metropolis [27] updating scheme which chooses new trial configurations by a random change in the direction of one single spin at the time. Our simulation has provided a new *visual* way of examining the physics in the XY model, and it gave us some unknown and interesting information about the system's behaviour in the non-equilibrium phase of the Monte Carlo simulations. When starting from an initial, random spin configuration, it appeared at low temperatures that the system always went through a vortex phase before settling in an equilibrium configuration, where the spins pointed all in very nearly the same direction. We also could see that the vortices disappeared only by drifting into others with opposite vorticity. This behaviour was not observed at higher temperatures.

Figure 4 shows snapshots of the terminal screen during a low temperature Monte Carlo simulation. The system is seen to start out from an initial, random configuration. Soon the spin configuration is dominated by the vortices, and they start annihilating by drifting into one

another. Figure 4b shows a configuration, close to equilibrium which contains few vortices. These persist due to the nature of the Metropolis Monte Carlo algorithm and also a consequence of the periodic boundary conditions. The Metropolis algorithm only checks the couplings to the nearest neighbours when trying to update a spin, and it is therefore a local updating algorithm. When we are at very low temperatures only configurations with lower energy will be accepted. This means that applying the algorithm can be thought of as combing a disordered, long-hair carpet. Because Metropolis only combs locally, it will start a local ordering of the spins all over the system, creating small domains of aligned spins. The ordering will gradually grow to bigger regions, and the vortices will show up. In the end all of the spins will have to be aligned at these low temperatures as in figure 4c, and the only way to get rid of the vortices is by combing oppositely charged pairs into one another.

In addition the vortex phase turned out to be very stable. It only took a few iterations to establish this phase, but many more were required to “comb out” the vortices into the smooth equilibrium spin configuration. The stability can be explained by the fact that the vortices appear as configurations having stationary energy with respect to variations of the field

$$\frac{\delta H[\phi]}{\delta \phi} = 0 \quad (16)$$

This means that the vortices become local potential wells, and by trying to get out of such a configuration one will almost always have to increase the energy of the system. It is then reasonable that we will need a considerable number of Monte Carlo steps to take the system out of these local energy minimum configurations into the equilibrium, global energy minimum.

We were also able to directly probe the Kosterlitz-Thouless prediction of the model having two different phases in equilibrium using the visual simulation. It appeared that the vortices exist only in tightly bound pairs below the critical temperature. As expected, we were able to detect free vortices above the critical temperature. Just above T_c the event of a vortex pair unbinding was very rare, but the unbinding clearly became more common as the temperature was increased further.

Figure 5 shows some equilibrium snapshots above and below T_c . The spins are here omitted in order to emphasize the vortex behaviour. In figure 5a we display a typical configuration below the critical temperature. Vortex pairs are spontaneously created and annihilated in pairs, and they always exist in pairs. For the case of a temperature above the critical temperature a different behaviour is observed, as shown in 5b. The vortices are also here created and annihilated in pairs, but we have here the possibility of a vortex pair unbinding. This event is very rare just above T_c , but it is more common at higher temperatures. The effect seems to be caused by other vortex pairs being created in between the original pair. These

other pairs are then polarized and thus screen off the interaction between the original pair, thereby making it easier for the original pair to unbind.

B. The two-dimensional XY model in a magnetic field

In this section we present the simulation of a model which is quantum mechanical in nature. To our knowledge there have been no previous attempts to construct a visual simulation of this model.

Superconductors exhibit the Meissner effect. In the superconducting phase an external magnetic field H will be repelled and within the superconductor the magnetic field is zero. In a type-I superconductor, upon increasing the external magnetic field, the superconducting state collapses at the critical field H_c and the applied field enters the material. But if the external field is now reduced the material re-enters the superconducting state at H_c , and the flux which had entered is expelled. This expulsion of the flux, the Meissner effect, would not occur for a perfect conductor. In a type-II superconductor flux first enters the superconductor in the form of quantized flux lines at a critical field H_{c1} , but the superconducting state does not collapse. As the applied field increases the density of flux lines increases until the system enters the normal state smoothly at the upper critical field H_{c2} . A $H - T$ phase diagram for a type-II superconductor is sketched in figure. 6.

The phenomenological Ginzburg-Landau theory of superconductivity has very successfully explained all the most important features of superconductivity [28]. It’s basic assumption is that a superconductor at each point in space is characterized by a complex order parameter $\psi(\mathbf{x})$

$$\psi(\mathbf{x}) = |\psi(\mathbf{x})| e^{i\phi(\mathbf{x})} \quad (17)$$

where $|\psi(\mathbf{x})|^2$ equals the density of superconducting Cooper pairs. There are two characteristic lengths in the Ginzburg-Landau theory. A magnetic field will penetrate a small distance into the superconductor, but vanishes at a distance $\sim \lambda$; the penetration depth. The coherence length ξ is roughly the distance over which the superconducting phase $\psi(\mathbf{x})$ varies from zero to it’s maximal value. A superconductor can be characterized by the Ginzburg-Landau parameter $\kappa = \lambda/\xi$. If $\kappa < 1/\sqrt{2}$ it is type-I, otherwise it is type-II. The high- T_c superconductors are of extreme type-II in the sense that the $\kappa \gg 1$. It was shown in a classic paper by Abrikosov [29] that the flux lines in a type-II superconductor will form a hexagonal lattice and this has also have been seen experimentally [30]. The dynamics of such a 3 dimensional flux-line or vortex lattice has been of considerable interest after the discovery of high temperature superconductors [31]. Based on experimental [32] and theoretical [33–35] results it was proposed that the flux-line lattice

melts into a vortex liquid over large parts of the $H - T$ phase diagram sketched in figure 6.

A widely used microscopic model [36–38] for describing the statistical mechanics of the flux line lattice is the XY model in a magnetic field with a Hamiltonian given by

$$H = - \sum_{ij} \cos(\phi_i - \phi_j - A_{ij}) \quad (18)$$

where ϕ_i is the phase of the superconducting wave function ψ at site i , the sum is over nearest neighbour sites and

$$A_{ij} = \frac{2e}{\hbar c} \int_i^j \mathbf{A} \cdot d\mathbf{l} \quad (19)$$

is the integral of the vector potential from site i to site j . This effective model can be derived by discretizing the Landau-Ginzburg free energy functional under the assumption of a spatial uniform magnetic induction and constant $|\psi|$ outside the normal vortex cores, the London approximation [39]. The flux lines are three dimensional objects, but in some cases it turns out to be a good approximation to treat them as two dimensional, i. e. as straight lines in the z direction. A superconducting thin film is one case and another is high- T_c superconductors which consist of weakly coupled layers, and so for some range of parameters may display effectively two dimensional behaviour [35,41]. In an extreme type-II superconductor the magnetic field, given by $B = \nabla \times A$, is to a good approximation uniform, when the magnetic penetration depth λ is larger than the inter vortex distance $a_0 \approx \sqrt{\Phi_0/B}$ must be much larger than the coherence length. In the Ginzburg-Landau theory, the lower and upper critical fields are given by $H_{c1} \approx \Phi_0/4\pi\lambda^2$ and $H_{c2} \approx \Phi_0/2\pi\xi^2$. For an extreme type-II superconductors $H_{c2}/H_{c1} \approx 2\xi^2 \gg 1$ and there is thus a wide field of the $H - T$ phase diagram of figure 6 for which the amplitude fluctuations can be neglected [40].

We consider a quadratic lattice with lattice constant a which serves as a measure of the coherence length ξ . Each flux line carries a flux equal the flux quantum $\Phi_0 = hc/2e$ and the average density of field induced vortices is thus $f = Ba^2/\Phi_0$. Since the total flux through a plaquette of the lattice equals $\oint \mathbf{A} \cdot d\mathbf{l}$, the sum over A_{ij} around such a square must obey the constraint

$$A_{ij} + A_{jk} + A_{kl} + A_{li} = 2\pi f \quad (20)$$

The localization of the vortices are as in the standard XY model determined by calculating the total change of the phase ϕ around a plaquette: $\sum_{\square} (\phi_i - \phi_j) = 2\pi n$, where n is the integer vorticity. Neither the phase ϕ nor the vector potential \mathbf{A} are directly observable quantities, but choosing a particular gauge fixes \mathbf{A} and thereby ϕ . However, it is convenient [37] to treat the model in a gauge invariant manner, and we will follow this approach. The

superconducting current density is a physical observable and can be expressed as

$$\mathbf{J} = |\psi(\mathbf{x})|^2 \frac{e\hbar}{m} \left(\nabla\phi - \frac{2e}{\hbar c} \mathbf{A} \right) \quad (21)$$

Hence the factor $\alpha_{ij} = \phi_i - \phi_j - A_{ij}$ of the Hamiltonian is gauge invariant. Throughout the simulations no reference is ever made to a specific vector potential, nor to a specific phase ϕ . The Monte Carlo moves are instead performed on the gauge invariant phase α which is the single dynamic variable of the system. As stated above, the vorticity depends on the phase difference of ϕ only. Nevertheless it is possible to calculate the vorticity from the gauge invariant phase α since

$$\sum_{\square} (\phi_i - \phi_j - A_{ij}) = 2\pi(n - f) \quad (22)$$

where the value of $\alpha_{ij} = \phi_i - \phi_j - A_{ij}$ is restricted to the interval $(\pi, -\pi)$.

One of the goals of Monte Carlo simulations of vortex lattices is to determine the phase diagram (see for instance figure 1 in [42]) including the pinned solid Abrikosov phase and a liquid phase as well as the depinned floating solid phase. For the latter the hexagonal lattice is intact, but it is not pinned and able to move as a whole. In the simulations this corresponds to a phase where the hexagonal lattice floats on the underlying numerical lattice. For such investigations it is very useful to be able to see how the actual configurations change during the simulations, for different temperatures and concentrations of vortices.

Here we will concentrate on the formation of a hexagonal Abrikosov lattice generated when starting from high temperature and relaxing at a sufficiently low temperature. For studies of the phase diagram it is essential that a hexagonal lattice can be formed at low temperatures without frustration. In actual simulations the size of the lattices is restricted by practical concerns and in order to approximate a large system better, periodic boundary conditions are imposed. If the appropriate size of the underlying numerical lattice is not carefully chosen, this will lead to frustration of an hexagonal lattice. Since we use a quadratic numerical lattice, a perfect hexagonal lattice can not be generated, and also a proper vortex concentration f must be chosen. The dilute case, $f \rightarrow 0$, can equivalently be viewed as the continuum limit, in which the lattice spacing a decreases to zero for a fixed areal density of vortices. So for addressing the problem of vortex lattice melting in a uniform superconducting film, the vortex concentration f should be small, probably less than $1/30$ in order to see all the three phases of the phase diagram. The ground state configurations are quadratic for large concentrations [43], even for $f = 1/25$ [44], and hence f must be smaller in order to approach the continuum limit.

These considerations are taken into account when choosing $f = 1/30$ on a lattice of 30×30 lattice sites

[45]. For these parameters an almost perfect hexagonal lattice may be formed without frustration due to periodic boundary conditions. As an initial state we choose the high temperature limit, a random configuration of vortices. It is possible to construct an algorithm which initiates the lattice with any given configuration of vortices by going sequentially through the lattice and assigning phases on the links according to Eq. 22, choosing $n = 1$ for a plaquette containing a vortex and $n = 0$ for plaquette containing none. After the initial configuration has been loaded, sites are chosen at random and probed by the Metropolis method. A trial configuration for a single Monte Carlo step is chosen by adding a random phase Δ to the links surrounding a site as shown in figure 8. A sequence of steps equal to the total number of lattice sites, 30×30 , is one iteration. During the first few iterations the vortex configuration changes rapidly and occasionally vortex anti-vortex pairs are created, as seen in figure 9a. Even vortices with a vorticity of two may occur in this chaotic phase of the simulation. After a large number of iterations an almost hexagonal lattice is formed, as seen in figure 9b. There are some fluctuations around this configuration because of the finite temperature, but the hexagonal lattice is pinned to the underlying numerical lattice and thus not moving. According to Ref. [45] one would expect the vortex lattice to melt into a vortex liquid when increasing the temperature above $T = 0.045$. At this temperature both the helicity modulus, a measure of long-range phase coherence, and the sixfold orientational order parameter drops rapidly to zero, which means that depinning and melting occurs at the same temperature.

However, if the vortex concentration is lowered to $f = 1/56$ the helicity modulus drops at $T_p = 0.03$ and the orientational order parameter at $T_m = 0.05$ [45]. This means that the system at T_p enters the floating solid state where the hexagonal vortex lattice is unpinned and moves as a whole independent of the numerical square lattice. The appearance of such a phase signals the onset of the continuum limit, since the pinned phase is an artifact of the lattice model. This is because there is a finite energy cost for displacing a vortex in the ground state configuration. At T_m the hexagonal lattice melts and the system finally enters the vortex liquid phase. A vortex concentration f of less than $1/30$ is therefore necessary in order to study the true melting of the flux lattice.

The gauge invariant phases α are also visualized in figure 9. The arrows show the positive direction of the phase (current) and their size is proportional to the magnitude of the phases. Close to the vortex core there are strong currents due to the rapid change of the superconducting phase ϕ . In between the vortices the current around a plaquette is small, but nonzero. Here there is no contribution from the superconducting phase, but there is a small net current in the opposite direction due to the constant magnetic field.

C. Diffusion into a lattice

In the previous examples the models were based exclusively on a square lattice in order to simplify special highlighting algorithms. In this section we wish to present a more generic automaton which demonstrates the adaptability of CASE's object oriented construction. We use a toy model for classical Brownian motion. The algorithm is intended to represent diffusion of particles into the surface plane of a crystalline lattice from outside. The plane being visualized should therefore be thought of as a surface layer separating a three dimensional region of solid crystal from a corresponding region of empty space filled with gaseous particles. When particles penetrate the lattice from the gaseous region they appear spontaneously in the model at a random site. When they leave lattice by further penetration into the bulk or by escaping back into the gaseous region they disappear from the model. This is used as a simple toy model which may be developed into a model for the way in which atomic hydrogen penetrates a palladium lattice.

The geometry of the lattice is completely hidden from the model algorithms and we can therefore run several simulations with different lattice structures side by side and compare them without having to rewrite any code whatsoever. It is not necessary to know the specifics about the background geometry: simple abstractions such as 'nearest neighbour' suffice. To determine possible destinations for particle hopping, we need only obtain a list of nearest neighbours from the lattice-specific object. Figure 10a illustrates the diffusion model implemented on a rectangular lattice, while figure 10b shows the same model on a triangular lattice. The difference between these images is a single switch: no special code is required in the model to make this change. Figure 10c shows a larger simulation with some background colour highlighting.

The dynamics of the model are derived from simple energy considerations. To make the model physically reasonable, we must have an exchange of energy and a Monte-Carlo based algorithm for randomly perturbing the system. For this simple demonstration we choose to illustrate an interaction between the thermodynamical properties of the lattice and the arrival and disappearance of particles. When a new particle enters the system, it contributes an amount of energy which warms up the lattice locally. This energy input is a combination of kinetic energy and energy of dissociation of a chemical bond as molecular hydrogen becomes atomized. The values of these energies are set to constant values in the model object. The extra heat contributed to the lattice is visualized by a change in the background colour from blue (cold) to green (warm). The change occurs locally, but on each iteration of the model, an averaging procedure is used to conduct away local hot spots and maintain thermal equilibrium. The colour of the particle blobs represents the energy of the particles and uses a dif-

ferent colour scale for clarity. The energy of the particles is chosen randomly for the sake of illustrating a variety of colours.

Particles are selected at random and can hop over to nearest neighbour sites with a certain probability; this introduces a Brownian motion into the system. The probability for hopping depends on an energy barrier or work function which we have chosen to scale according to the square root of the average temperature between nearest neighbour sites. This crudely simulates a classical harmonic barrier of height x where $\frac{1}{2}kx^2 = k_B T$. Thus increased thermal activity of the lattice makes diffusion harder at constant particle energy. The following code snippet illustrates a simple Brownian motion algorithm using the lattice independent mechanisms.

```
// Find the nearest neighbours at 1-st level
// by querying lattice

grid->QueryNeighbours(i, 1, neighbours);

for (i = 0; i < neighbours.GetSize(); i++)
{
    if (neighbours.array[i] == environ->NoCell)
    {
        continue; // Edge effect
    }

    neigh = (ThermoCell *) cell[neighbours.array[i]];

    if (neigh->Alive())
    {
        continue;
    }

    // Get energy for required processes

    beta = Tscale / (current->T + neigh->T);

    transition_prob =
        exp(-beta*Work(neigh,current,cell_index,i));

    // Note 'least action'

    if (transition_prob > highest)
    {
        highest = transition_prob;
        favourite = neighbours.array[i];
    }
}

// If we have no free neighbour sites

if (highest == 0.0)
{
    return;
}

// Move if the roulette wheel favours the wicked ...
```

```
if (highest >= drand48())
{
    neigh = (ThermoCell *) cell[favourite];
    current->SetAlive(False);
    neigh->SetAlive(True);
    neigh->E = current->E;
    Draw(cell_index);
    Draw(favourite);
}
```

Notice how we avoid referring to the specific details of the lattice by only using the lists of neighbours which are returned by the QueryNeighbours function.

As one would expect in a thermalizable system, equilibrium is achievable here after a number of iterations. The escape of a particle from the lattice is possible if it can borrow enough thermal energy from the local lattice site, with a certain probability which may be defined in the model. This results in a local cooling of the lattice. The higher the temperature of the lattice, the greater the probability of escape. In figure 10c one sees lighter areas of locally higher temperature. After a certain time one sees the equilibration in relation to the environmental parameters in the model. The number of particles in the lattice stabilizes: as the temperature increases and evens out, the likelihood of particles escaping increases.

VI. CONCLUSIONS

We have presented a framework for simultaneously visualizing and computing numerical quantities from cellular or lattice simulations, using a scheme of abstractions which faithfully separates independent issues. Our framework is based on an object oriented analysis of the key elements of physical systems on a lattice. As an example we present the *XY* model for electron spins at finite temperature and show the approach to thermal equilibrium in both the vortex phase and the ferromagnetic phase. Using the visual simulation it is possible to see the Kosterlitz-Thouless phase transition in this model: tightly bound pairs of vortices below a critical temperature, and vortex unbinding above the critical temperature. We are further able to visualize the gauge invariant currents surrounding quantum mechanical vortices in a magnetic field. A toy model for diffusion illustrates the lattice independence possible in some cases.

Our computer programs are suitable for unix workstations running release 6 of the X11 window system (Linux or FreeBSD for instance). More information about how to collect and adapt these simulations may be found at the WWW site <http://www.iu.hioslo.no/~cell>. We may also be contacted by email at case@iu.hioslo.no.

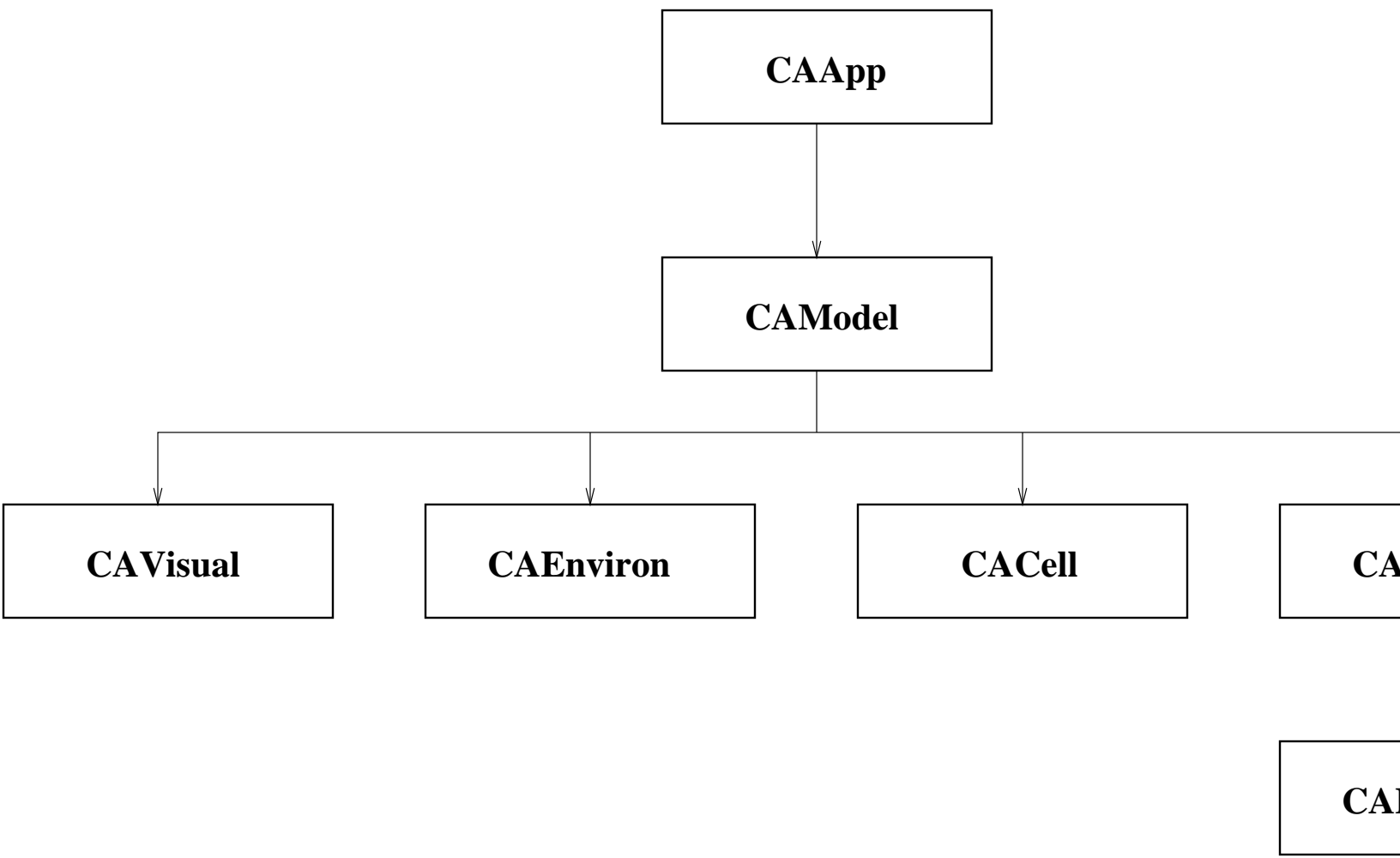
Acknowledgments

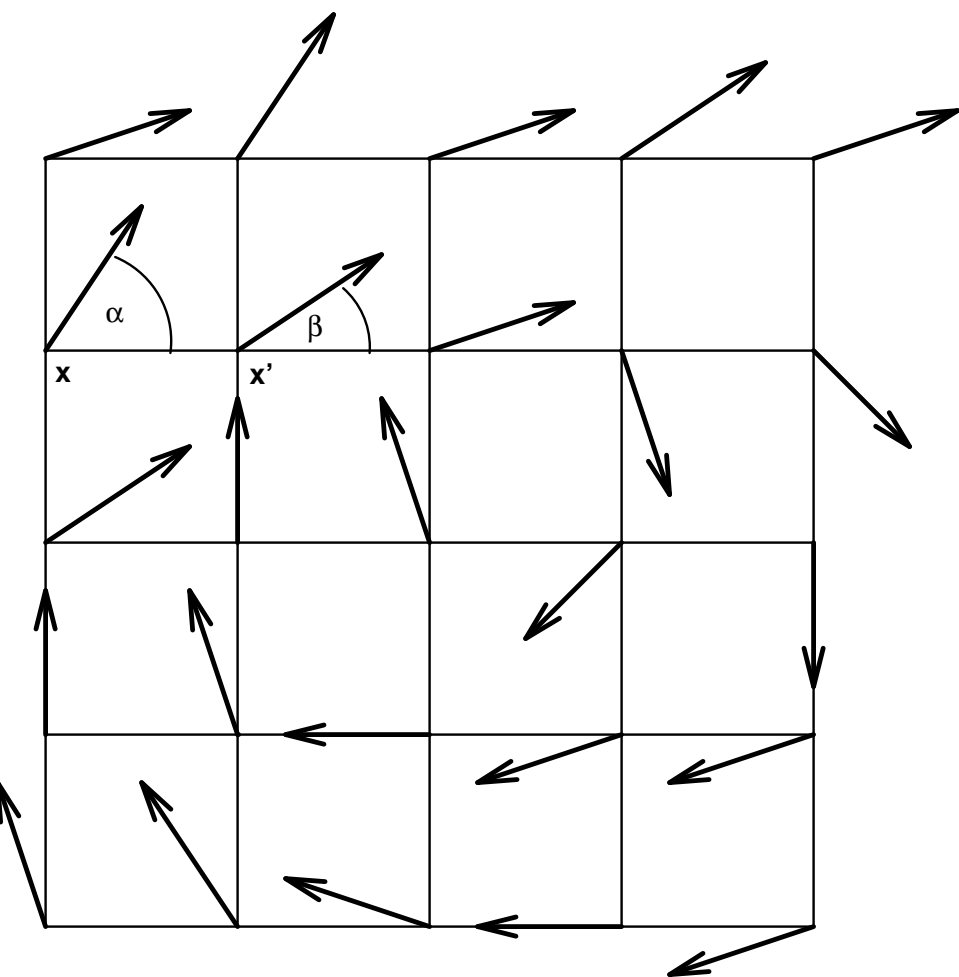
We would like to thank F. Ravndal for stimulating this visualization project and A. Sudbø for introducing us to the interesting idea of visualizing the XY model in external magnetic field. We also very much like to draw attention to the essential contributions made by J. Mikkelsen and T.E. Sevaldrud in the design and implementation of the CASE library as part of their dissertation in computer science at Oslo College.

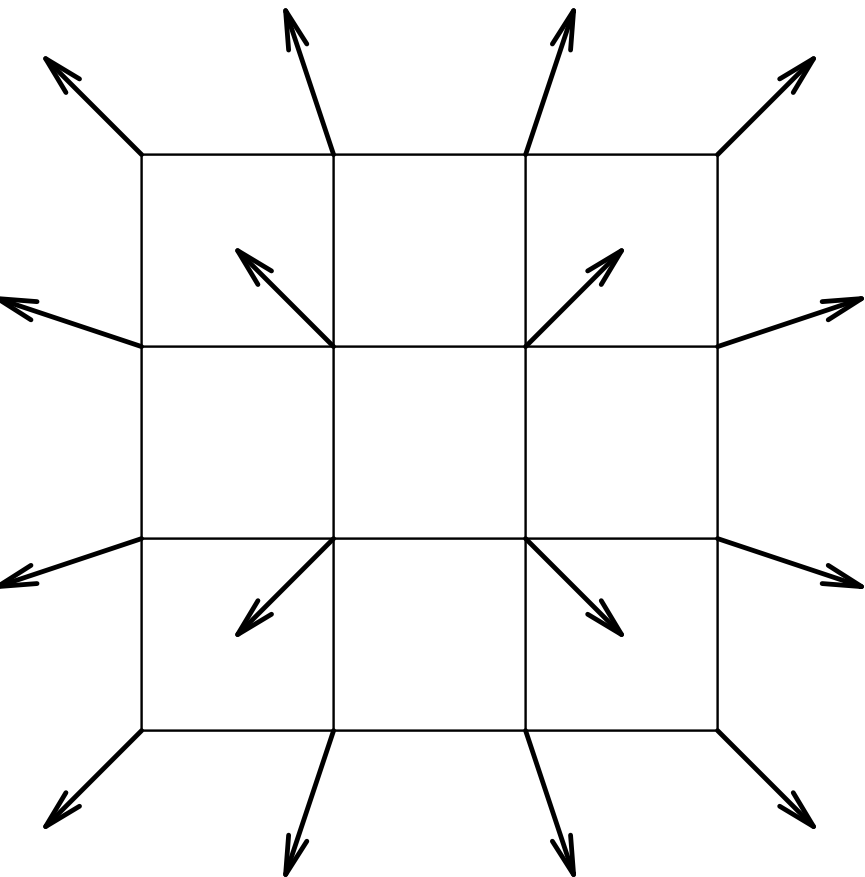
-
- [1] See for collected papers, F. Wilczek (ed), *Fractional statistics and anyon superconductivity*, World Scientific, Singapore (1990)
- [2] For a review, see: A. Karlhede, S.A. Kivelson and S.L. Sondhi, *The quantum Hall effect: The Article*, Lectures presented at the 9th Jerusalem Winter School on Theoretical Physics (1992).
- [3] R. Feynman, *Simulating physics with computers*, Int. J. Theor. Phys. Vol **21**, 467, 1982
- [4] B.P. Zeigler, *Discrete event models for cell space simulation*, Int. J. Theor. Phys. Vol **21**, 573, 1982
- [5] M. Minsky, *Cellular Vacuum*, Int. J. Theor. Phys. Vol **21**, 537, 1982
- [6] K. Zuse, *The computing universe*, Int. J. Theor. Phys. Vol **21**, 589, 1982
- [7] A. Schadscheider and M. Schreckenberg, *Cellular automata for traffic flow*, cond-mat/9511037, LANL database.
- [8] E. Dan Dahlberg and J.G. Zhu, *Micromagnetic Microscopy and Modelling*, Physics Today April 1995, 34.
- [9] The Argus project, <http://www.geog.le.ac.uk/argus/About/aboutargus.html>
- [10] The Virtual Laboratory, <http://www.tp.umu.se/TIPTOP/VLAB/about.html>
- [11] B.E. Kane et al., Phys Rev B**46**, 7264 (1992); M. Johnson, Appl. Phys. Lett. **63**, 1435 (1993); M. Johnson, Phys Rev Lett**70**, 2142 (1993); M. Burgess and M. Carrington, Phys. Rev. B**52**, 5052, (1995).
- [12] S. Wolfram, *Cellular automata and complexity*, Addison Wesley (1994)
- [13] M. Suzuki in *Physics of Low-Dimensional Systems*, Proceedings of Koyoto Summer Institute, edited by Y. Nagaoka and S. Hikami (Publication Office, Prog. Theor. Phys., Kyoto, 1979) p. 39
- [14] T. Matsubara and H. Matsuba, *Prog. Theor. Phys.* **16** (1956) 416; T. Matsubara and H. Matsuba, *Prog. Theor. Phys.* **17** (1957) 19
- [15] P. Minnhagen, *Rev. Mod. Phys.* **59** (1987) 1001
- [16] Y. E. Lozovik and S. G. Akapov, *Solid State Commun.* **35** (1980) 693
- [17] J. Tobochnik and G. V. Chester, *Phys. Rev. B* **20** (1979) 3761
- [18] N. Schultka and E. Manousakis, *Phys. Rev. B* **49** (1994) 12071
- [19] *The Monte Carlo Method in Condensed Matter Physics*, Ed. K. Binder, Springer Verlag Berlin Heidelberg (1992)
- [20] T. Tokihiro, D. Takahashi, J. Matsukidaira and J. Satsuma, *Phys. Rev. Lett.* **76** 3247 (1996)
- [21] Note that our code is constructed in such a way as to make this restriction removable at a later time.
- [22] Our XY simulation was first demonstrated publicly at the 1994 workshop on anyon physics, Norway.
- [23] The X window system, volumes 0 - 10, O'Reilly and Associates.
- [24] J.A. Mikkelsen and T.E. Sevaldrud, *Cellular automaton simulation environment*, Ing. dissertation, Oslo college, Centre of Science and Technology (1996).
- [25] There are several available tools for mathematical modeling: Mathematica, Maple, IDL etc, but these are commercial programs designed for a much wider purpose than we require, and are therefore inefficient for numerical iteration combined with graphics. Also the new language Java turns out to be too slow and not sufficiently mature to be useful for our purposes, moreover they cannot handle the abstractions which CASE uses for modelling a physical environment.
- [26] J. M. Kosterlitz and D. J. Thouless, *J. Phys. C* **6**, 1181 (1973)
- [27] N. Metropolis, A. Rosenbluth, M. Rosenbluth, A. Teller and E. Teller, *J. Chem. Phys.* **21** (1953) 1087
- [28] M. Tinkham, *Introduction to Superconductivity* McGraw-Hill (1975)
- [29] A. A. Abrikosov, *Zh. Eksp. Teor. Fiz.* **32** (1957) 1442
- [30] U. Essmann and H. Träuble, *Phys. Lett.* **24A** (1967) 526
- [31] For reviews, see G. Blatter et al., *Rev. Mod. Phys.* **66** (1994) 1125; E. H. Brandt, *Rep. Prog. Phys.* **58** (1995) 1465
- [32] P. L. Gammel, L. F. Schneemeyer, J. V. Wasczczak and D. J. Bishop, *Phys. Rev. Lett.* **61** (1988) 1666
- [33] D. R. Nelson, *Phys. Rev. Lett.* **60** (1988) 1973
- [34] A. Houghton, R. A. Pelcovits and A. Sudbø, *Phys. Rev. B* **40** (1989) 6763
- [35] D. S. Fisher, M. P. A. Fisher and D. A. Huse, *Phys. Rev. B* **43** (1991) 130
- [36] Y.-H. Li and S. Teitel, *Phys. Rev. Lett.* **66** (1991) 3301
- [37] R. E. Hetzel, A. Sudbø and D. A. Huse, *Phys. Rev. Lett.* **69** (1992) 518
- [38] M. Franz and S. Teitel, *Phys. Rev. B* **51** (1995) 6551
- [39] Y.-H. Li and S. Teitel, *Phys. Rev. B* **47** (1993) 359
- [40] A. Sudbø and E. Brandt, *Phys. Rev. B* **43** (1991) 10482
- [41] L. I. Glazman and A. E. Koshelev, *Phys. Rev. B* **43** (1991) 2835
- [42] S. A. Hattel and J. Wheatly, *Phys. Rev. B* **50** (1994) 16590
- [43] S. Teitel and C. Jayaprakash, *Phys. Rev. Lett.* **51** (1983) 1999
- [44] Y.-H. Li and S. Teitel, *Phys. Rev. B* **49** (1994)
- [45] S. A. Hattel and J. Wheatly, *Phys. Rev. B* **51** (1995) 11951

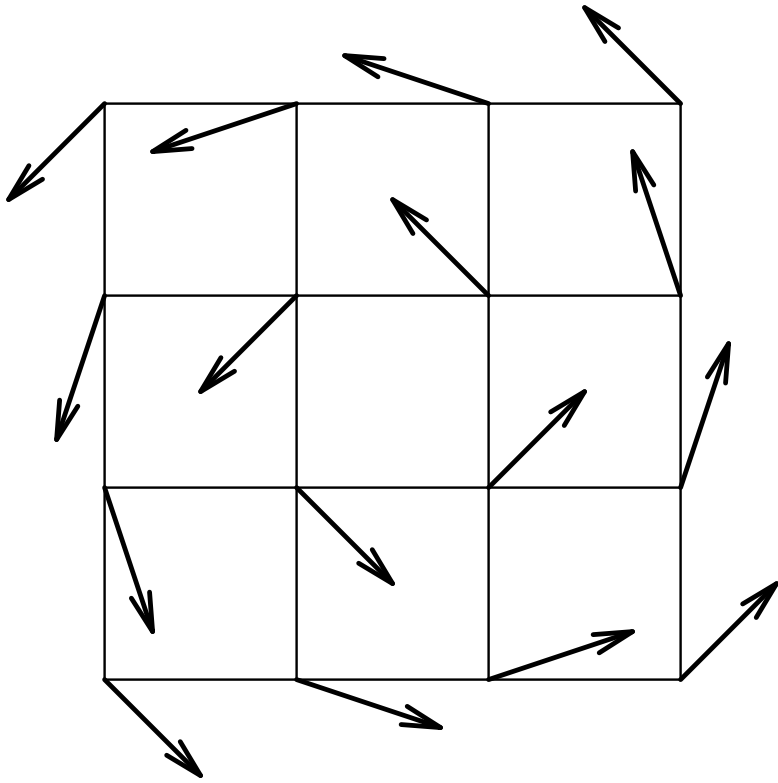
VII. FIGURE CAPTIONS

1. The CASE object hierarchy.
2. A 5×5 lattice with spins. The sites \mathbf{x} and \mathbf{x}' are indicated. Here $\phi_{\mathbf{x}} - \phi_{\mathbf{x}'} = \alpha - \beta$.
3. Vortices in the XY model: (a) All spins point in the direction away from the vortex core. (b) The spins have all been rotated an angle $\pi/2$. This whirl-shape is a characteristic of a vortex.
4. This figure shows the route into equilibrium at $T = 0.1$ for the XY model.
5. Equilibrium snapshots at $T = 0.8$ and $T = 1.0$. The vortices are seen to exist mostly in bound pairs. An example of vortex unbinding is shown in b).
6. The phase diagram of a type-II superconductor.
7. The characteristic lengths of the model. While the coherence length ξ equals the lattice spacing, the magnetic penetration depth λ is supposed to be much larger than the inter vortex distance.
8. When choosing a trial configuration a random phase Δ is added to the phases α of the four links connected to the probed site in this manner. This corresponds to adding the phase Δ to the superconducting phase ϕ at the site, which ensures that Eq. 22 is always fulfilled and thus that the magnetic flux through the four neighbouring plaquettes remains unchanged.
9. Snapshots of the XY model in a magnetic field. (a) Shows an initial disordered state of the system (b) Shows the state of the system after a large number of iterations, where an almost hexagonal lattice of the vortices is formed. (c) An enlarged portion of the figure in (b) obtained by zooming in on the lower right hand corner with the middle mouse button, a standard function in the CASE library.
10. Snapshots of the thermodiffusion simulations: a) shows the model implemented on a square lattice, (b) shows the model on a triangular lattice and c) illustrates the behaviour of the colour highlighting in the triangular case after some time.









This figure "fig4a.gif" is available in "gif" format from:

<http://arxiv.org/ps/cond-mat/9707007v1>

This figure "fig4b.gif" is available in "gif" format from:

<http://arxiv.org/ps/cond-mat/9707007v1>

This figure "fig4c.gif" is available in "gif" format from:

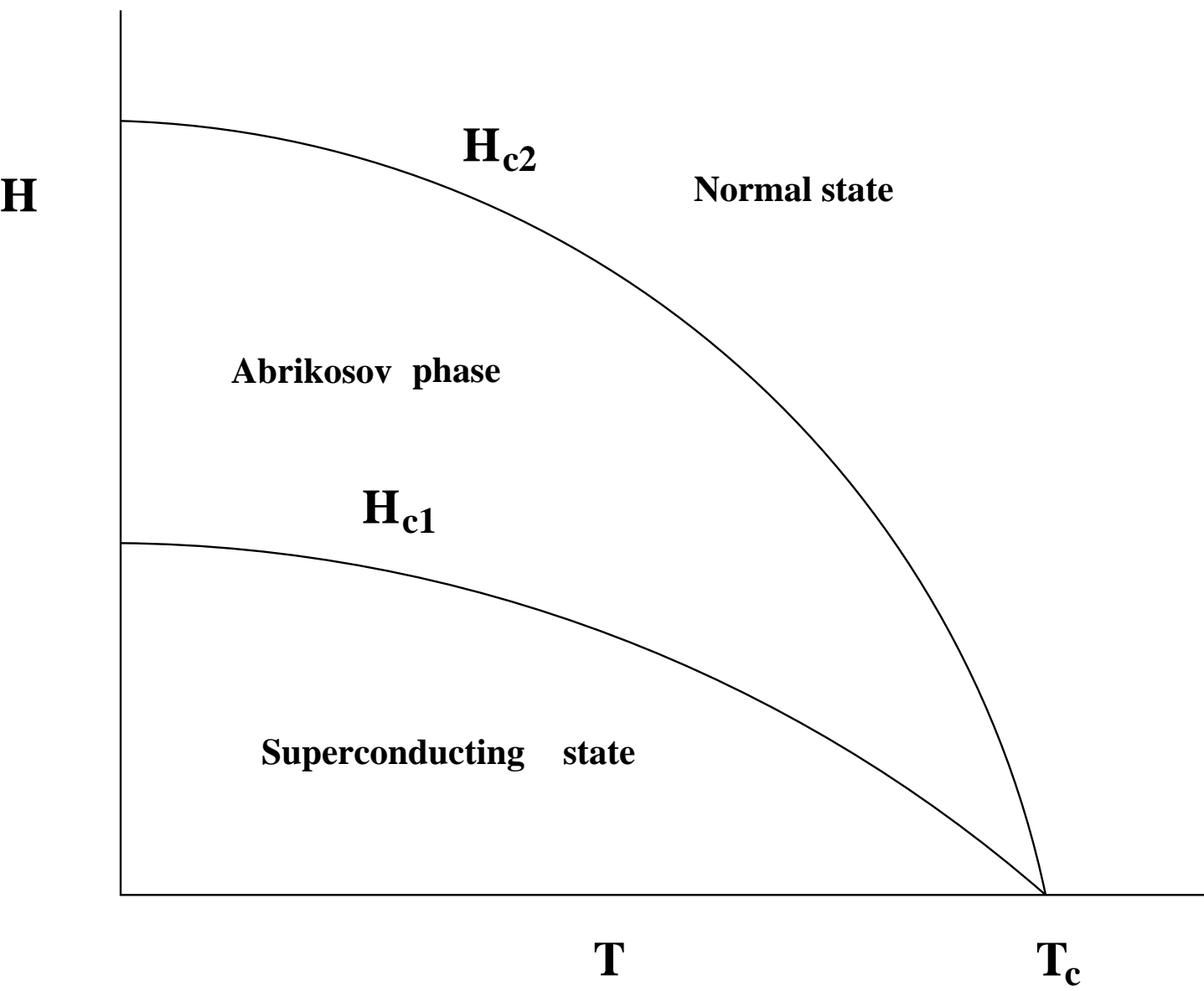
<http://arxiv.org/ps/cond-mat/9707007v1>

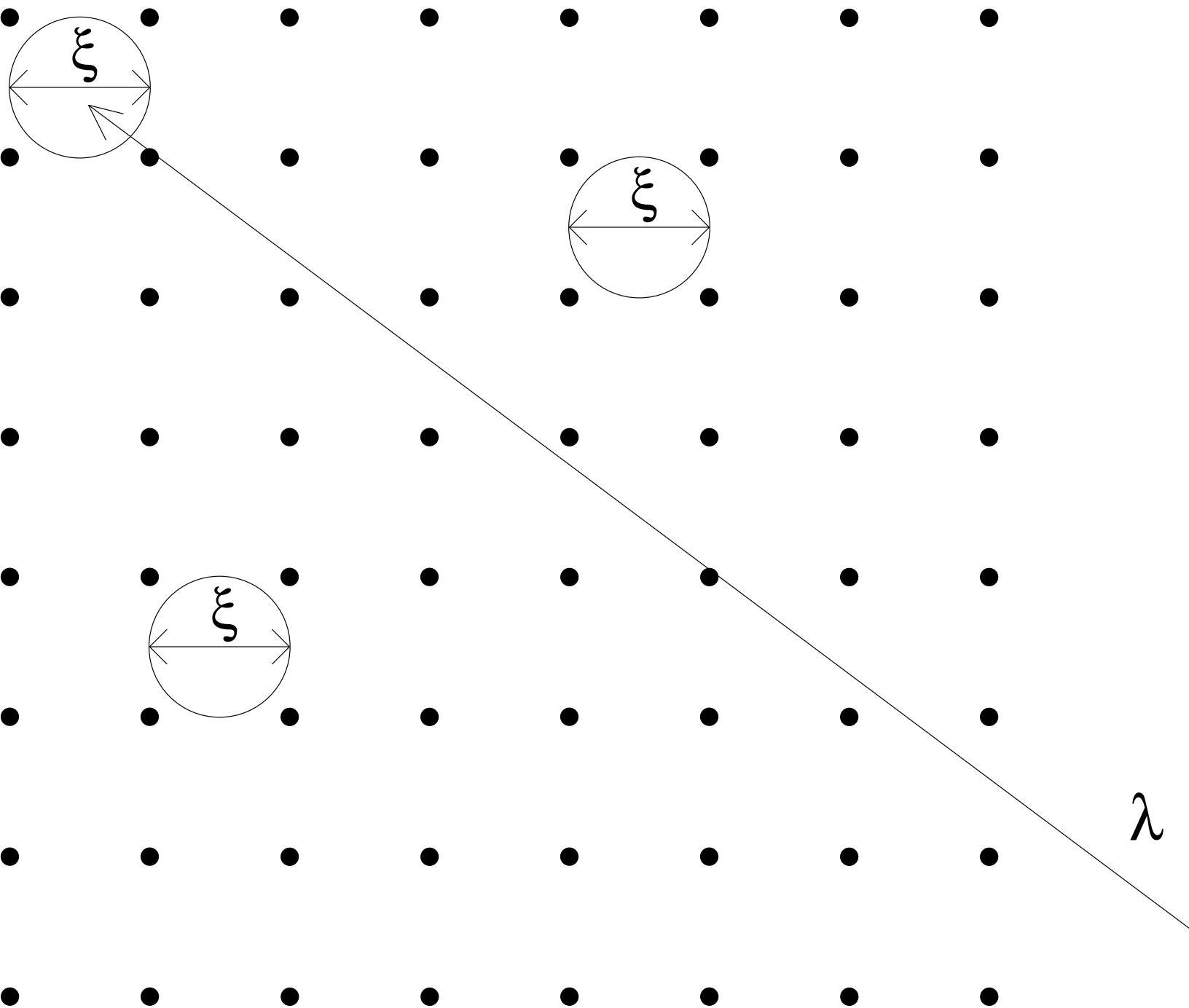
This figure "fig5a.gif" is available in "gif" format from:

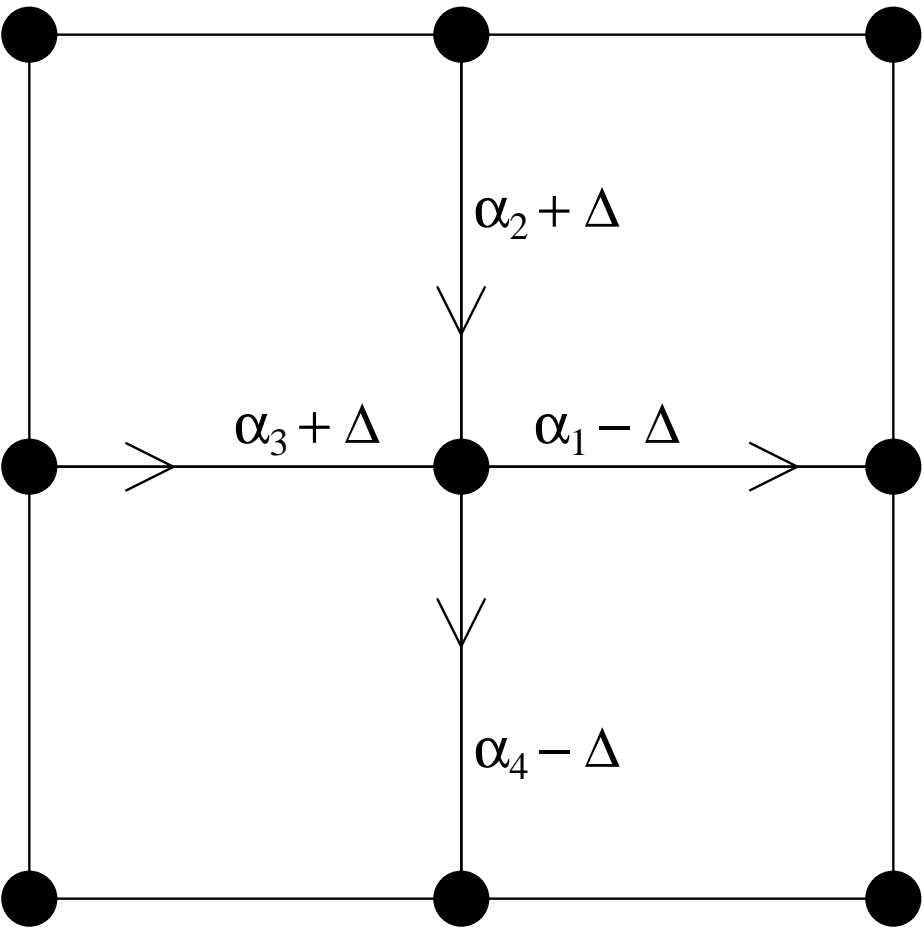
<http://arxiv.org/ps/cond-mat/9707007v1>

This figure "fig5b.gif" is available in "gif" format from:

<http://arxiv.org/ps/cond-mat/9707007v1>







This figure "fig9a.gif" is available in "gif" format from:

<http://arxiv.org/ps/cond-mat/9707007v1>

This figure "fig9b.gif" is available in "gif" format from:

<http://arxiv.org/ps/cond-mat/9707007v1>

This figure "fig9c.gif" is available in "gif" format from:

<http://arxiv.org/ps/cond-mat/9707007v1>

This figure "fig10a.gif" is available in "gif" format from:

<http://arxiv.org/ps/cond-mat/9707007v1>

This figure "fig10b.gif" is available in "gif" format from:

<http://arxiv.org/ps/cond-mat/9707007v1>

This figure "fig10c.gif" is available in "gif" format from:

<http://arxiv.org/ps/cond-mat/9707007v1>